

# Tunneling spectroscopy of the normal-state gap in $(\text{Bi,Pb})_2\text{Sr}_2\text{Ca}_2\text{Cu}_3\text{O}_{10+\delta}$

Toshikazu Ekino\*

Faculty of Integrated Arts and Sciences, and Graduate School of Advanced Sciences of Matter, Hiroshima University,  
Higashi-Hiroshima 739-8521, Japan

Satoru Hashimoto and Tomo'aki Takasaki

Department of Quantum Matter, Graduate School of Advanced Sciences of Matter, Hiroshima University,  
Higashi-Hiroshima 739-8526, Japan

Hironobu Fujii

Faculty of Integrated Arts and Sciences, Hiroshima University, Higashi-Hiroshima 739-8521, Japan

(Received 7 June 2000; revised manuscript received 7 December 2000; published 14 August 2001)

Tunneling spectra have been measured on as-grown  $(\text{Bi,Pb})_2\text{Sr}_2\text{Ca}_2\text{Cu}_3\text{O}_{10+\delta}$  with  $T_c = 110$  K using a ceramic break junction. The superconducting-gap size is in scale with that of as-grown  $\text{Bi}_2\text{Sr}_2\text{CaCu}_2\text{O}_{8+\delta}$  ( $T_c = 86$  K). The closing temperatures  $T^*$  of the normal-state gap are found to be  $\approx 170$  and  $\approx 250$  K, which are similar to  $T^*$  of Bi2212. The tunneling conductance displays a distinction between the superconducting gap and the normal-state gap around  $T_c$ . Near room temperature, the zero-bias conductance enhancement is observed, which could reflect the energy-gap spectrum with a different conduction mechanism from tunneling (e.g., the Andreev scattering).

DOI: 10.1103/PhysRevB.64.092510

PACS number(s): 74.72.Hs, 74.50.+r, 74.25.Jb, 74.80.-g

There are numbers of experimental evidences for the gap creation above the superconducting transition temperature  $T_c$  in the copper oxides.<sup>1-6</sup> Such a gap is considered to be due to the spin gap, the pairing fluctuation, the charge/spin density wave, or the charge stripe formations.<sup>7-9</sup> Intensive studies have been made on  $\text{Bi}_2\text{Sr}_2\text{CaCu}_2\text{O}_{8+\delta}$  (Bi2212) to elucidate its origin.<sup>2-6</sup> The intercalated Bi2212 has been also investigated, in which the  $\text{CuO}_2$  bilayer is believed to be responsible for the normal-state gap creation.<sup>6</sup> Since  $\text{Bi}_2\text{Sr}_2\text{Ca}_2\text{Cu}_3\text{O}_{10+\delta}$  (Bi2223) is one of the homologous series of  $\text{Bi}_2\text{Sr}_2\text{Ca}_{n-1}\text{Cu}_n\text{O}_{4+2n+\delta}$  ( $n$  denotes the numbers of  $\text{CuO}_2$  layers per unit cell), the existence of normal-state gap is also expected. Further, the possible difference in the antiferromagnetic coupling constant  $J$  between Bi2212 ( $n=2$ ) and Bi2223 ( $n=3$ ) would result in the difference in energy scales of the normal-state gap in terms of magnetic origin.<sup>10</sup> The measurements of Bi2223 should be therefore effective to insight into the underlying mechanism of the normal-state gap. However, only a few tunneling measurements have been available on this compound.<sup>11,12</sup>

In this paper, we investigate the normal-state gap in Bi2223 to address this issue. The polycrystals of  $\text{Bi}_{2-x}\text{Pb}_x\text{Sr}_2\text{Ca}_2\text{Cu}_3\text{O}_{10+\delta}$  ( $x \approx 0.1, y < 0.5$ ) are used for the experiment, which were grown by a solid-state reaction. Tunneling measurements were done using the break junction with a four-probe method. The sample was cracked at  $T = 77$  K to find the stable gap feature near  $T_c$ .

Figure 1 shows the tunneling conductance for Bi2223 taken from several different junctions at 77.3 K ( $T/T_c \approx 0.7$ ). In the inset, the  $T$  dependence of the resistivity  $\rho$  and the deviation from its linearity is shown. The  $T_c$  ( $\rho=0$ ) = 110 K is obtained, which is consistent with that from the predominant onset of decrease in the susceptibility. The curves A and B possess the well-defined outer humps which look similar to the other break junction<sup>4,5</sup> and interlayer tunneling results,<sup>6</sup> while the curves C, D, and E are quite differ-

ent from these data. The inner gap edge peaks at  $\pm 63$ –68 mV corresponds to  $\pm 2\Delta/e$  of the superconductor-insulator-superconductor (SIS) junction, where  $2\Delta$  is the superconducting energy gap defined by half the peak-to-peak separation ( $V_{p-p}$ ) in the conductance. The gap value of  $\Delta$  (77.3 K) = 32–34 meV is consistent with  $\Delta$  (4 K) = 37–39 meV,<sup>11</sup> and it is also in scale with that of as-grown (slightly overdoped) Bi2212.<sup>4</sup> In the curves C–E, only the single gap is observed. The bias positions of their conductance peaks coincide with either the superconducting-gap edge (C) or the outer humps (D and E) of A and B. The gap-edge peaks of D and E are broadened as compared with the superconducting-gap edge of A and B. These large variations of gap size might be due to intergrain tunneling with different crystallographic orientations. Nevertheless, the re-

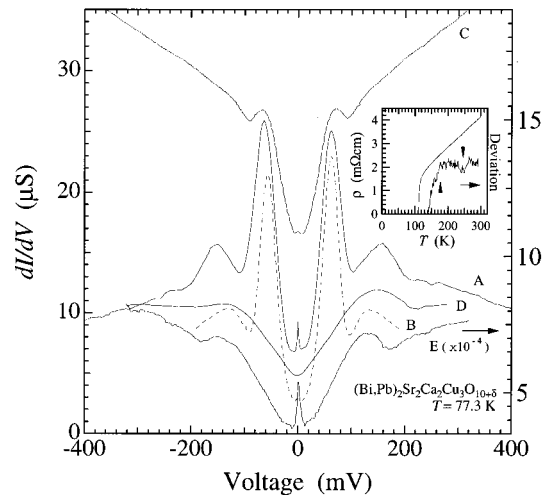


FIG. 1. Tunneling conductance for Bi2223 at 77.3 K taken from different break junctions. The inset shows the  $T$  dependence of the resistivity  $\rho(T)$  and its deviation from the linearity.

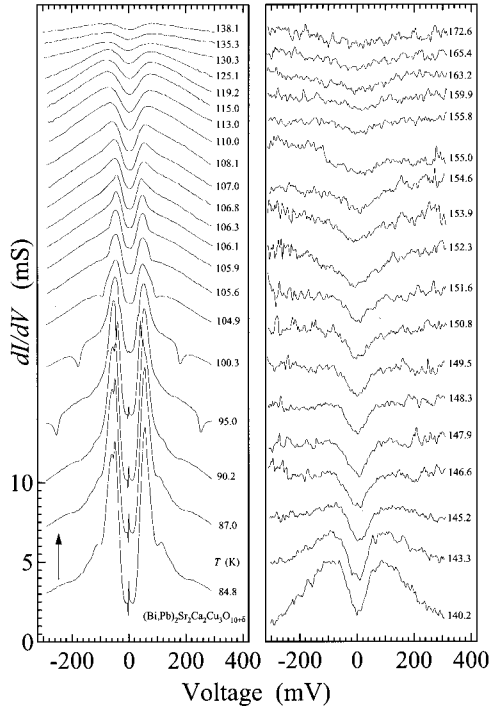


FIG. 2. Temperature variations of the tunneling conductance for a Bi2223 break junction.

producible two distinct biases of  $\pm 60$ – $70$  mV and  $\pm(160 \pm 30)$  mV are observed as in the case of Bi2212 single crystal.<sup>13,14</sup> Therefore, the above phenomenon seems to be not the case. The observation of the single gap indicates that the double-peak structure in A and B is probably not inherent to the superconducting density of states. Further, the single-gap feature of D and E with the energy corresponding to that of outer humps of the superconducting gap is seen close to room temperature in both break-junction and interlayer-tunneling spectra.<sup>6,14</sup> This suggests that the origins of the superconducting gap and the outer humps are different. One of the origins of the larger gap causing the outer hump structure can be associated with the semiconducting gap of Bi-O layers.<sup>15–17</sup>

Figure 2 shows  $T$  variations of the tunneling conductance taken from another junction. In our measurements, the width of the tunneling barrier could not be kept constant with the change in  $T$  because of the thermal expansion of the junction. However, once a stable junction is formed at low  $T$ , the magnitude of high-bias conductance varies slowly upon warming, while the zero-bias dip is filled quickly reflecting the thermal reduction of the gap. In the figure, the Josephson peak completely disappears at  $T_c = 106$  K, but the gap feature still persists beyond  $T_c$  where the gap edge becomes sharp. Just above  $T_c$ , the gap-edge broadening and the gap-width expansion occur simultaneously. Upon further warming, the ingap state is gradually filled with the well-defined gap edge up to  $\approx 150$  K, and then it merges into the background at the gap-closing temperature  $T^* \approx 170$  K. This value is similar to  $\approx 180$  K of as-grown Bi2212.<sup>5</sup> For  $T > T^*$ , the background conductance is almost flattened.

To evaluate the tunneling data, we have carried out the

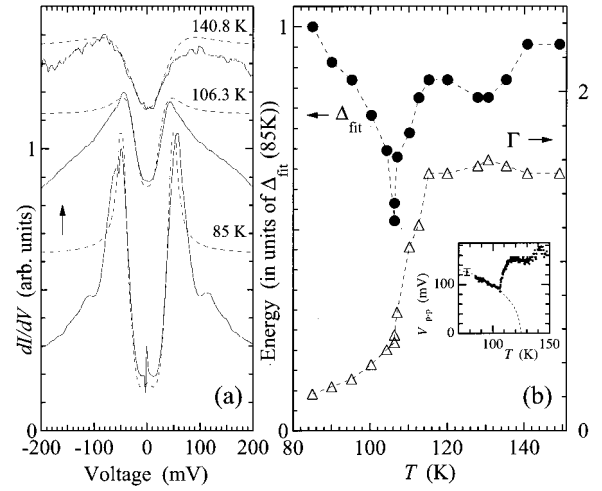


FIG. 3. (a) Comparison between the conductance of Fig. 2 (solid line) and  $N(E, \Delta_{\text{fit}}, \Gamma, T)$  (broken line) (Ref. 18). No mutual vertical offsets for each comparison. (b) Temperature dependence of the fitted gap  $\Delta_{\text{fit}}$  and  $\Gamma$  obtained from the above fitting. The inset shows the temperature dependence of the conductance-peak separation  $V_{p-p}$  obtained from Fig. 2. The dotted line represents the BCS prediction.

conductance fitting assuming the broadened BCS density of states  $|\text{Re}\{(E - i\Gamma)/[(E - i\Gamma)^2 - \Delta_{\text{fit}}^2]\}|$  with thermal smearing  $[=N(E, \Delta_{\text{fit}}, \Gamma, T)]$ , where  $\Delta_{\text{fit}}$  and  $\Gamma$  are the fitted gap value and a phenomenological broadening parameter, respectively.<sup>18</sup> Although the use of  $N(E, \Delta_{\text{fit}}, \Gamma, T)$  for the superconducting gap of Bi2223 is not guaranteed theoretically, the substantial agreements have been obtained in the case of the homologous Bi2212.<sup>13</sup> In the normal state, there is also no justified density-of-states model. Nevertheless, we try to fit to examine whether it is applicable or not. Figure 3(a) shows the representative fitting results in the  $T$  region below and above  $T_c$ . The ingap conductance is fairly well reproduced by  $N(E, \Delta_{\text{fit}}, \Gamma, T)$  with appropriate  $\Delta_{\text{fit}}$  and  $\Gamma$  at a given  $T$ , where no mutual conductance offsets are given in both the experimental and calculated curves. This means that the leakage conductance of this tunnel junction is almost due to the density-of-states broadening with  $\Gamma$ . The disagreement outside the gap could be reduced using the normalized conductance by the background. The fitting parameters, however, are similar because of the weak bias dependence of the ingap background. If the gap anisotropy is averaged out by the intergrain tunneling, the V-shaped gap should be observed at low  $T$ ,<sup>19</sup> but this is not the case here.

In Fig. 3(b), the  $T$  dependence of  $\Delta_{\text{fit}}$  and  $\Gamma$  is shown. At 85 K,  $4\Delta_{\text{fit}} \approx 100$  meV almost agrees with  $V_{p-p} \approx 115$  mV. The  $\Gamma$  is much smaller than  $\Delta_{\text{fit}}$  below  $T_c$ , but it becomes comparable to  $\Delta_{\text{fit}}$  at  $T_c$ . It begins to increase quickly just above  $T_c$  to become  $\Gamma > \Delta_{\text{fit}}$ , and eventually saturates at  $\Gamma \approx 1.5\Delta_{\text{fit}}$  above  $\approx 115$  K. The rapid increase of  $\Delta_{\text{fit}}$  above  $T_c$  on warming with the large increase of  $\Gamma$  is remarkable. This is probably not solely due to the increasing normal-state sample resistance  $R_s$  because of  $R_s[\approx 500 \Omega (300 \text{ mV})] \gg R_s (< 1 \text{ m}\Omega)$  and only the  $\Gamma$  is largely different across  $T_c$ . The condition  $\Gamma > \Delta_{\text{fit}}$  for  $T > T_c$  implies incoherent or non-

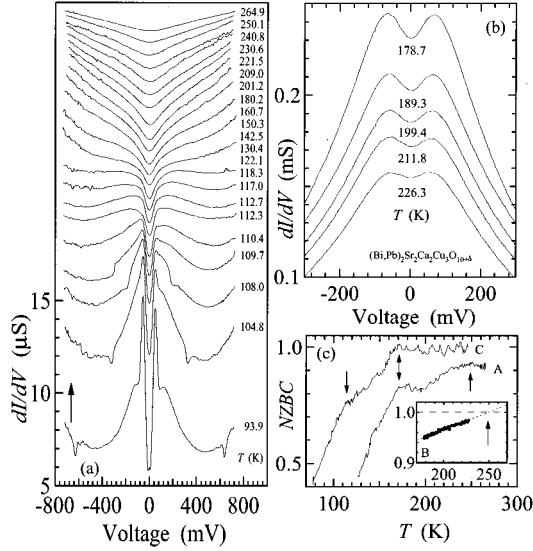


FIG. 4. (a) and (b) Temperature variations of the tunneling conductance from different Bi2223 break junctions. (c) Temperature dependence of the normalized zero-bias conductance  $NZBC(T)$ . The curves A (a), B (b), and C are taken from the different junctions.

bulk nature of the gap, which also might suggest the formation of the different kind of density of states from that below  $T_c$  with  $\Gamma < \Delta_{fit}$ . The inset of Fig. 3(b) shows the  $T$  dependence of the model-independent  $V_{p-p}$ . With increasing  $T$ , the  $V_{p-p}$  decreases to take a minimum at  $T_c = 106$  K and then increases to saturate at  $\approx 115$ – $120$  K. In the narrow  $T$  interval near  $T_c$ , the  $V_{p-p}$  changes rapidly. The structure again occurs at  $\approx 130$  K. The behavior of  $V_{p-p}(T)$  roughly resembles the sum of  $\Delta_{fit}(T)$  and  $\Gamma(T)$ . The  $T$  of  $\approx 120$ – $130$  K agrees with the extrapolated gap-closing temperature  $T_c^{ex} = 125$  K using a BCS dependence.<sup>12</sup> This means that the superconducting gap remains finite at  $T_c = 106$  K though it is assumed to eventually disappear at  $T_c^{ex}$ . In fact, a weak break in  $\rho(T)$  is observed at  $\approx 125$  K.<sup>20</sup> The recent photoemission measurements of Rast *et al.*<sup>21</sup> obtained the similar results to ours, in which they argue the competing  $T$  dependence of the gap in terms of two different order parameters of the electronic phase transitions. Such a competition has been also predicted by the calculation assuming the coexistence of the superconductivity and CDW.<sup>8</sup> When we assume the precursor superconductivity above  $T_c$ , the competing crossover near  $T_c$  might suggest the different pairing symmetries below and above  $T_c$ .

Figure 4(a) shows  $T$  variations of tunneling conductance up to near room temperature with much higher biases. The  $R_J$  is much higher ( $\approx 10^2$ – $10^3$ ) than that of Fig. 2. The conductance background becomes a V shape above  $\approx 120$  K. The gap feature diminishes at  $T^* \approx 170$ – $180$  K, remaining a weak zero-bias depression which merges into the background at  $\approx 230$ – $250$  K. In Fig. 4(b), the well-defined gap edge is visible at least up to  $\approx 226$  K using the different junction. The  $T$  dependence of the normalized zero-bias conductance,  $[NZBC(T)]$  in Fig. 4(c) exhibits the gap disappearance more clearly. The  $NZBC(T)$ , which is defined as

the gap depth divided by the high-bias ( $\approx 500$  mV) conductance, is introduced to reduce the effect of the thermal expansion thus the barrier width of the junction. This is based on the fact that the thermal variations of the conductance at zero bias is much larger than that at high biases. Using this procedure, the thermal evolution of the electronic properties can be separated from the thermal expansion of the junction.<sup>22</sup> The curves A and B are taken from (a) and (b), respectively, while the C from another junction not presented here. Every  $NZBC(T)$  demonstrates the increasing trend with  $T$  in accordance with the thermal filling up of the gap. The distinct steplike structures occurring at  $\approx 110$  and  $\approx 170$  K in A and C correspond to  $T_c$  and  $T^*$ , respectively. The additional subtle break is visible at  $\approx 130$ – $140$  K for A and C, and the gradual depression below  $\approx 250$  K for A. The former temperature is probably related with  $T_c^{ex}$  as discussed in Fig. 3, while the latter is consistent with the extrapolated  $T^* \approx 250$  K of B. The substantial variations in  $T^*$  with the reproducible superconducting gap size and  $T_c$  among the examined junctions indicate that the  $T^*$  variations are not closely related to the change in the doping rate responsible for the bulk superconductivity below  $T_c$ . The similar reproducible values of  $T^* \approx 170$  and  $\approx 250$  K are also observed in as grown Bi2212.<sup>5,14</sup> These observations seem to be incompatible with the prediction that  $T^*$  would scale between Bi2212 ( $n=2$ ) and Bi2223 ( $n=3$ ) compounds arising from the possible difference in  $J[J(n=3) > J(n=2)]$ .<sup>10</sup> These common values of  $T^* = 170$  and  $\approx 250$  K against the systematic difference in  $T_c$  (and the superconducting gap) between the compounds with  $n=2$  and  $3$  could be explained in terms of the local order parameters from the particular electronic phases. In fact, the abrupt depression of  $NZBC(T)$  just below  $T^*$  resembles that for the gap due to the electronic phase transition,<sup>5,14</sup> though it is not due to the bulk phenomenon. From the reduction in  $NZBC(T)$ , the volume fraction of the gapped phase just above  $T_c$  could be estimated as  $\approx 3$ – $4\%$ . Actually, only very subtle structures corresponding these  $T^*$  are visible in the deviation of  $\rho(T)$  from the linearity (Fig. 1 inset). The higher  $T^*$  of  $\approx 250$  K has been also reported in  $\rho(T)$  of Bi2223 whiskers as the upturn deviation from the  $\rho(T)$  linearity.<sup>23</sup> The existence of the higher-order ( $n > 3$ ) homologous intergrowths in the main phase could produce the behavior of  $NZBC(T)$ , as in Fig. 4(c) which shows multiple transitions, as has been observed in the susceptibility on this kind of compound.<sup>24</sup> Further, these  $T^*$  values are found to agree with the characteristic temperatures of the incoherent lattice fluctuations in  $YBa_2Cu_3O_{7-\delta}$ ,<sup>25</sup> which might suggest the existence of the common characteristic temperatures in the normal-state electronic phases of the copper-oxide superconductors.

Figure 5 shows evidence for the distinction of the superconducting gap and the outer humps. The superconducting gap disappears at  $T_c$ , while the outer humps stay almost unchanged across  $T_c$  to become single gap above  $T_c$ . This feature is in contrast to Fig. 2 but is rather similar to Fig. 4(a). The gap is still clearly seen at  $284.2$  K. The variations of the crossover behaviors in Figs. 2, 4(a), and 5 suggest the existence of the different kinds of the normal-state gaps or

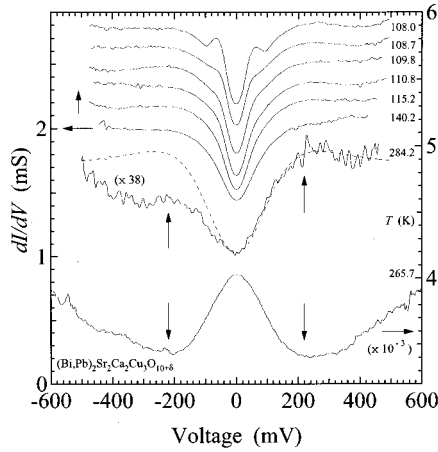


FIG. 5. Tunneling conductance at  $\approx T_c$  and near room temperature. The broken line for the 284.2 K data represents  $N(E, \Delta_{\text{fit}}, \Gamma, T)$  (Ref. 18).

the different control parameters for their appearances.<sup>14</sup> By considering the results of intrinsic interlayer (*c*-axis)-tunneling measurements on Bi2212 showing the coexistence of the superconducting gap and the normal-state gap,<sup>6</sup> the interface geometry of the junction may be responsible for the differences observed here. To evaluate the shape of the gap at 284.2 K, the conductance is fitted by  $N(E, \Delta_{\text{fit}}, \Gamma, T)$  with SIS tunneling. The dashed curve is obtained with  $\Delta_{\text{fit}} = 90$  meV and  $\Gamma = 100$  meV. The condition  $\Gamma > \Delta_{\text{fit}}$  implies incoherent nature of the normal-state gap. The calculated curve agrees with the experimental one for the positive bias without any vertical offset, indicating that the conductance leakage comes from the broadening of the gap. The asymmetry in the conductance is probably due to the charge imbalance or the rectification at the junction.

In addition to the normal-state tunneling gap, we have observed the broad zero-bias hump near room temperature

by readjusting the junction (Fig. 5 bottom curve). In the superconducting state, such a hump is attributed to the weak link or the Andreev scattering at the junction.<sup>26</sup> However, the present case is in the normal state. Nevertheless, the occurrence of the Andreev-like scattering arising from the pair formation within the correlation length near the interface cannot be excluded, because the bias positions of the conductance minima agrees with those for the gap energy, and the hump displays a moderate magnitude  $\approx 20\%$  for such a phenomenon. The Andreev scattering in the normal-state phase-incoherent (or local phase-coherent) pairings can in fact occur.<sup>27</sup> On the other hands, the Andreev scattering from CDW or SDW is perhaps not the case because it may exhibit the depression of the zero-bias conductance owing to the electron-hole condensation.<sup>27</sup> Such a zero-bias hump also can be caused by the low-dimensional electronic states arising from the charge-stripe formation.<sup>9</sup> Other possibilities, such as normal-metallic weak link at the junction causing the Joule heating, series resistance consisting of chains of inhomogeneous grains, resonant tunneling, etc., also could cause a zero-bias hump, but these seem to be unlikely because the conductance minima occur exactly at the gap-edge energy with moderate change in the conductance. Further, we observe such a zero-bias hump only for the fresh-and-clean break junction condition, indicating that this feature comes from the intrinsic electronic properties of the material.

In summary, we present tunneling measurements of the normal-state gap of as-grown Bi2223(*n*=3) ceramics using the break junction. The reproducible  $T^*$  values below room temperature are found to be  $\approx 170$  and  $\approx 250$  K. The coexistence of the superconducting gap and normal-state gap is also observed around  $T_c$ . These features are similar to those of as-grown Bi2212(*n*=2), supporting the idea that the superconducting gap and the normal-state gap are not directly related each other. Near room temperature, the gap structure as well as the zero-bias conductance enhancement are observed, which would deserve to further investigation in terms of the possible pairing formation.

\*Corresponding author. E-mail address: ekino@hiroshima-u.ac.jp

<sup>1</sup>H. Ding *et al.*, Nature (London) **382**, 51 (1996).

<sup>2</sup>Ch. Renner *et al.*, Phys. Rev. Lett. **80**, 149 (1998).

<sup>3</sup>Y. I. Latyshev *et al.*, Phys. Rev. Lett. **82**, 5345 (1999).

<sup>4</sup>N. Miyakawa *et al.*, Phys. Rev. Lett. **80**, 157 (1998).

<sup>5</sup>T. Ekino *et al.*, Phys. Rev. B **60**, 6916 (1999).

<sup>6</sup>A. Yurgens *et al.*, Int. J. Mod. Phys. B **13**, 3758 (1999); V. M. Krasnov *et al.*, Phys. Rev. Lett. **84**, 5860 (2000).

<sup>7</sup>V. J. Emery and S. A. Kivelson, Nature (London) **374**, 434 (1995).

<sup>8</sup>M. V. Eremin *et al.*, Physica B **259–261**, 456 (1999).

<sup>9</sup>V. V. Moshchalkov *et al.*, Europhys. Lett. **46**, 75 (1999).

<sup>10</sup>D. Munoz *et al.*, Phys. Rev. Lett. **84**, 1579 (2000).

<sup>11</sup>Q. Chen *et al.*, Phys. Rev. B **49**, 6193 (1994).

<sup>12</sup>T. Ekino *et al.*, J. Low Temp. Phys. **117**, 359 (1999).

<sup>13</sup>Ya. G. Ponomarev *et al.*, Physica C **315**, 85 (1999); S. I. Vedenev *et al.*, Phys. Rev. B **49**, 9823 (1994).

<sup>14</sup>T. Ekino *et al.*, J. Phys. Chem. Solids **62**, 149 (2001).

<sup>15</sup>T. Haswgawa and K. Kitazawa, Jpn. J. Appl. Phys. **29**, L434 (1990).

<sup>16</sup>Y. Sezaki, T. Ekino, and H. Fujii, Physica B **259–261**, 555 (1999).

<sup>17</sup>C. Howard, P. Fournier, and A. Kapitulnik, cond-mat/0101251 (unpublished).

<sup>18</sup>R. C. Dynes, V. Narayanamurti, and J. P. Garno, Phys. Rev. Lett. **41**, 1509 (1978).

<sup>19</sup>L. Ozyuzer *et al.*, Phys. Rev. B **57**, 3245 (1998).

<sup>20</sup>C. H. Kao *et al.*, Physica C **235–240**, 483 (1994).

<sup>21</sup>S. Rast *et al.*, Europhys. Lett. **51**, 103 (2000).

<sup>22</sup>T. Ekino *et al.*, Phys. Rev. B **53**, 5640 (1996).

<sup>23</sup>W. Chen *et al.*, Phys. Rev. B **60**, 3527 (1999).

<sup>24</sup>R. Schilling *et al.*, Nature (London) **363**, 56 (1993).

<sup>25</sup>R. P. Sharma *et al.*, Nature (London) **403**, 736 (2000).

<sup>26</sup>T. M. Klapwijk *et al.*, Physica B **109–110**, 1657 (1982).

<sup>27</sup>H. Y. Choi *et al.*, Phys. Rev. B **61**, 9748 (2000).